

COMPUTATIONAL APPROACH TO DARK CURRENT SPECTROSCOPY IN CCD AS COMPLEX SYSTEMS. PART III*. DEFINITION AND USE OF A NEW PARAMETER CHARACTERIZING THE DEPLETION DARK CURRENT IN SEMICONDUCTORS

I. TUNARU¹, R. WIDENHORN², E. BODEGOM², D. IORDACHE³

Rezumat. Studiul efectuat a evidențiat faptul că frecvent rezultatele experimentale privind vitezelor de generare ale principalelor capcane adânci nu corespund valorilor prezise de aproximația „clasică” (presupunând egalitatea secțiunilor eficace: $\sigma_n = \sigma_p$ de captură a electronilor liberi și – respectiv – golurilor) a modelului riguros cuantic al lui Shockley-Read-Hall (SRH). Pentru a îmbunătăți precizia descrierii curenților de întuneric de golire, lucrarea de față a introdus un nou parametru „gradul de polarizare a secțiunilor eficace de captură a electronilor liberi, respectiv golurilor”. În afara capacității sale de a furniza evaluări mai exacte ale curenților de întuneric din semiconductori, noul parametru reprezintă un instrument util pentru: a) analiza unor „anomalii” ale valorilor vitezelor de generare, b) atribuirea capcanelor cu nivele adânci pentru fiecare pixel CCD, pornind de la dependența de temperatură a curenților de întuneric din dispozitivele CCD.

Abstract. The accomplished study pointed out that frequently the experimentally observed generation rates of the main deep-level traps do not correspond to the values predicted by the classical approximation (assuming equal capture cross-sections $\sigma_n = \sigma_p$ of the free electrons and holes, respectively) of the Shockley-Read-Hall (SRH) rigorous quantum expression. In order to improve the accuracy of the depletion dark current description, this work introduced the new parameter “polarization degree of the capture cross-sections of free electrons and holes, respectively”. Besides its ability to provide considerably more accurate evaluations of the depletion dark current in semiconductors, this new parameter represents a useful tool for: a) the analysis of some “anomalies” of the generation rate values, b) the assignment of deep-level traps for each CCD pixel, starting from the experimental data concerning the temperature dependence of the dark current in CCDs.

Keywords: Charge-Coupled Devices, Dark Current, Capture cross-sections of free electrons and holes, Deep-level traps

1. Introduction

As it is well-known, the temperature dependence of the depletion dark current $De_{dep}^-(T)$ emitted in a semiconductor [with the intrinsic Fermi level E_i the

¹Ph.D. student, Physics Department, University “Politehnica” of Bucharest, Romania.

²Professor, Portland State University, Oregon, USA.

³Professor, Ph.D., Physics Department, University “Politehnica” of Bucharest, Romania, Honorary member of Academy of Romanian Scientists.

*This paper represents the continuation (3rd part) of the works indicated by references [16].

generation-recombination centers (or traps) characterized by the energy level E_t , the capture cross-sections σ_n, σ_p of free electrons and holes, respectively, and the concentration N_t] is described by the famous rigorous quantum expression of Shockley, Read and Hall [1–3], by means of the generation rate $U(T)$:

$$\frac{De_{dep}^-}{x_{dep}A_{pix}} = U(T) = \frac{\sigma_n \sigma_p V_{th} (p \cdot n - n_i^2) N_t}{\sigma_n \left[n + n_i \exp\left(\frac{E_t - E_i}{kT}\right) \right] + \sigma_p \left[p + n_i \exp\left(\frac{E_i - E_t}{kT}\right) \right]}, \quad (1)$$

where x_{dep} is the width of the depletion region, A_{pix} is the area of the pixel, and n_i is the intrinsic carrier concentration. Given being that besides the numerous physical parameters involved by expression (1), the temperature dependence of the depletion dark current due to the semiconductor lattice defects or impurities includes also the parameters describing the temperature dependence of all physical quantities from relation (1), it results that the use of this (too intricate) expression requires to consider some particular cases.

The most important such particular case refers to the region depleted of carriers, where n and $p \ll n_i$. In this case, the expression of the depletion dark current becomes:

$$I_{dep} = q \cdot x_{dep} A_{pix} \frac{\sigma_n \sigma_p V_{th} n_i N_t}{\sigma_n \exp\left(\frac{E_t - E_i}{kT}\right) + \sigma_p \exp\left(\frac{E_i - E_t}{kT}\right)}. \quad (2)$$

From relation (2), one finds [4] that the depletion dark current reaches a sharp maximum for the traps with energy:

$$\left(\frac{dI_{dep}}{dE_t} \right)_{E_t, \max I_{dep}} = 0 \rightarrow E_t = E_i - \frac{kT}{2} \ln \frac{\sigma_n}{\sigma_p}. \quad (3)$$

Taking into account that the trap energy level E_t and its capture cross-sections of free electrons σ_n and holes σ_p , respectively, are independent quantities, the quantities $\frac{E_t - E_i}{kT}$ and $\frac{1}{2} \ln \frac{\sigma_n}{\sigma_p}$ are not strictly equal, but they have to be of the same magnitude order for the detectable traps by means of the Dark Current Spectroscopy Method (DCS) [4, 5].

For this reason, the usual procedure (see e.g. [4, 6], relation (7.8), page 610) is to take into consideration $\frac{E_t - E_i}{kT}$ and neglect $\ln \frac{\sigma_n}{\sigma_p}$:

$$U(T) = \frac{\sigma \cdot V_{th} n_i N_t}{\exp \frac{E_t - E_i}{kT} + \exp \frac{E_i - E_t}{kT}} \quad (\text{where: } \sigma = \sigma_n = \sigma_p) \quad (4)$$

is not rigorous and cannot lead usually to accurate evaluations.

2. Check of the classical approximation (4) relative to the experimental results concerning the generation rate

The specialty literature provides (e.g. the works [5]) a sufficient number of experimental data about the generation rates of different deep level traps in silicon, pointing out even the existence of some still unexplained irregularities: “... there is actually more *Au* present on the *Mn* scribe line ... than there is *Mn*, although the stronger *Mn* trap dominates the dark current” [5c], p. 478.

For this reason, we studied the predicted – by means of approximation (4) – ratios $U_{\text{exp}} (e^- / s) \cdot \cosh \left[\frac{E_t - E_i}{kT_{\text{ave}}} \right] / \sigma$, which should be [according to relation (4)] almost equal for all traps. The obtained results were synthesized by Table 1.

Table 1. Calculated values (in the frame of this work) of the “invariant” [according to relation (4)]

$$U_{\text{exp}} (e^- / s) \cdot \cosh \left[\frac{E_t - E_i}{kT_{\text{ave}}} \right] / \sigma, \text{ proportional to the ratio } U_{\text{exp}} / U_{\text{theor}}$$

Trap	Generation rate $U_{\text{exp}} (e/s \text{ at } 55^\circ\text{C})$	Trap level $ E_t - E_i $ (meV) [5c]	Average cross-section σ (cm ²) [5c]	$U_{\text{exp}} (e^- / s) \cdot \cosh \left[\frac{E_t - E_i}{kT_{\text{ave}}} \right] / \sigma$
Mn	6400	$\sim < 50$	$\sim 1 \times 10^{-15}$	31074.0
Ni; Co	3700	< 30	6.6×10^{-15}	1161.5
Pt	970	60	7×10^{-15}	1051.0
Au _s	565	< 30	1×10^{-15}	1170.6
Fe _i	195	120 ÷ 150	3×10^{-14}	1461.5
Trap 1 (acceptor E-center)	70	100	2×10^{-15}	1615.2
Trap 2	8	200	8×10^{-15}	4258.3
Trap 3 (donor E-center)	1.8	270	2×10^{-14}	9100.6

One finds that the approximation (4) leads to evaluations of the generation rate:

(i) of the same magnitude order for *Ni*, *Co* and *Au* (especially), as well as (though sensibly different) for the *Pt*, *Fe_i*, and the acceptor E-center traps,

(ii) considerably smaller (almost 30 times) than the experimental results for the *Mn* traps,

(iii) sensibly smaller, but not so low as for *Mn*, for the traps 2 (unidentified) and 3 (donor E-center).

As it results from the more recent [7] studies of the *Mn* traps in *Si*, the most important causes of their striking strange overall behavior (see Table 1 and [5c]) are:

a) the large number of *Mn* defects types in *Si*: at least 4 different interstitial charge states *Mn_i*, other 3 different substitutional charge states *Mn_s*, those of the cluster *Mn₄*, those of the *Mn-metal* (*B*, *Al*, *Ga*, *Sn*, *Au*) pairs (at least 2 charge states *Mn-B*, 2 charge states of *Mn-Au*, etc ; see fig. 3),

b) the huge values interval of the capture cross-sections corresponding to the different charge states of *Mn* defects: starting from $\sigma_p = 2 \times 10^{-18} \text{ cm}^2$ for the $E_v + 0.27 \text{ eV}$ state of *Mn_i*, passing through the value $\sigma_n = 3.1 \times 10^{-15} \text{ cm}^2$ for the $E_c - 0.12 \text{ eV}$ and $E_c - 0.43 \text{ eV}$ states of *Mn_i* [8], up to $\sigma_n = 2.1 \times 10^{-12} \text{ cm}^2$ for the level located in proximity of the Fermi level in *Si* [7a], the value $\sigma \sim 10^{-15} \text{ cm}^2$ indicated by McColgin [5c] being in fact a geometric average of the *Mn* defects capture cross-sections over this extremely broad interval.

According to the conclusions of the [7a] work: "... *Mn* shows a far more complex defect structure than *Fe* or *Cr* for instant, which do not normally exist in the substitutional form and also exhibit one single interstitial energy level in the *Si* band gap. A consequence of these additional energy levels for *Mn* is that is difficult to state a priori which level dominates recombination, as the populations of the various charge states will depend on the Fermi level, i.e. on the doping type and concentration". It results that the approximation (4) should be replaced by a considerably more accurate one, which will be of special interest for the other deep-level traps (*Ni*, *Co*, *Pt*, *Au_s*, and even for the *Fe_i* and the acceptor E-center trap).

3. Definition of the new parameter "polarization degree of capture cross-sections"

Instead of the above approximation, this work has written (without any additional approximation) the expression (2) as:

$$I_{dep} = q \cdot x_{dep} A_{pix} \frac{\sqrt{\sigma_n \sigma_p} \cdot V_{th} n_i N_t}{2} \sec h \left[\frac{E_t - E_i}{kT} + pdg \right], \quad (5)$$

where $\operatorname{sech}(x)$ is the hyperbolic secant function: $\operatorname{sech}(x) = \frac{1}{\cosh x}$. (6)

The new parameter “polarization degree of the capture cross-sections of free electrons and holes, respectively” (pdg), describing the asymmetry of the pair of capture cross-sections σ_n, σ_p was defined by this work as:

$$p \equiv pdg = \arg \tanh \frac{\sigma_n - \sigma_p}{\sigma_n + \sigma_p} \equiv \frac{1}{2} \ln \frac{\sigma_n}{\sigma_p} \quad (7)$$

Figure 1 below presents the plots of the function $\operatorname{sech}(x+p)$ for different values of the variable x and of the parameter p of the magnitude order of 1. Taking into account the considerable deviations from the values of the previous factor $\operatorname{sech}\left[\frac{E_t - E_i}{kT}\right]$ of the function $\operatorname{sech}\left[\frac{E_t - E_i}{kT} + pdg\right]$, even for the very-deep level traps detectable by the DCS method, significant corrections of the depletion dark current evaluations are expected to be brought by the expression (5).

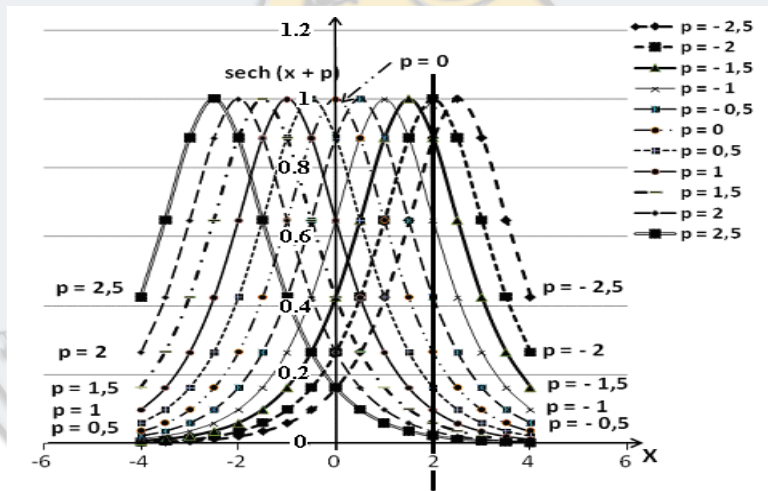


Fig. 1. Plots of the hyperbolic secant function $\operatorname{sech}(x+p)$ for different values of the parameters $x = (E_t - E_i)/(kT)$ and $p \equiv pdg$ (polarization degree of the capture cross-sections).

The thick vertical line through $x = +2$ indicates the descent of the $\operatorname{sech}(x+p)$ function from the value +1 for $p = -2$, up to less than +0.05 for $p = +2.5$.

¹The traps of the crystalline lattice (embedded nano-particles/systems, nano-defects) capture both free electrons and holes, but with different probabilities. Given being the capture probability is proportional to the corresponding cross-section (σ_n or σ_p), the capture probability asymmetry can be given by the expression (7) [somewhat similar to those from Optics, Nuclear physics, etc.], because: $pdg > 0$ corresponds to prevalent free electrons capture, $pdg = 0$ to equal capture probabilities, etc.

4. Existing experimental results about both capture cross-sections (of free electrons and holes, respectively) and their polarization degree (*pdg*)

Despite: a) the high technical interest presented by the identification of contaminants (see e.g. [5], [6]), b) the possibility to determine experimentally both capture rates for a given trap (by means of the DLTS method [9], especially), in practice there were evaluated: (i) usually up only the (geometrical) averages $\sigma = \sqrt{\sigma_n \sigma_p}$, (ii) both capture cross-sections only for a part of the different studied traps. Table 2 synthesizes some known values of both capture cross-sections of free electrons and holes, respectively, by certain defects (traps) from silicon, as well as of their polarization degree (*pdg*), implicitly. In order to understand easier the location of the different defects (traps) in Si, instead to indicate their positions relative to the upper limit of the valence band (E_v) or to the bottom limit of the conduction band (E_c), we give in Table 2 the evaluated traps energies relative to the intrinsic Fermi level, considered as $E_i \approx 0.54$ eV [4].

Table 2. Some known values of both capture cross-sections of free electrons and holes, respectively, in silicon, as well as of their polarization degree (*pdg*), implicitly

Trap	Group	Energy (eV)	σ_n (cm ²)	σ_p (cm ²)	$k = \sigma_n/\sigma_p$	<i>pdg</i>	Ref.	U (55°C) e/s [5c]
Ti_i^+	4	$E_i + 0.27$	3.1×10^{-14}	1.4×10^{-15}	22.14	+1.549	[7d]	
Ti_i^{++}	4	$E_i - 0.28$	1.3×10^{-14}	2.8×10^{-17}	464.3	+3.070	[7d]	
V_i^{++}	5	$E_i - 0.18$	5.0×10^{-14}	3.0×10^{-18}	16667	+4.86	[7d]	
Cr_i^{++}	6	$E_i + 0.32$	2.3×10^{-13}	1.1×10^{-13}	2.091	+0.369	[7d]	
		$E_i + 0.30$	2.0×10^{-14}	4.0×10^{-15}	5	+0.805	[10a]	
$(Cr_i^+ B_s^-)$	6; 13	$E_i - 0.26$	5.0×10^{-15}	1.0×10^{-14}	0.5	-0.3466	[10a]	
Mo_i^+	6	$E_i - 0.26$	1.6×10^{-14}	6.0×10^{-16}	26.67	+1.642	[10b]	
		$E_i - 0.223$	7.8×10^{-15}	6.0×10^{-16}	13	+1.282	[8b]	
Mn_i^+	7	$E_i + 0.09$			9.4	+1.1204	[7a]	
$(Mn_i^+ B_s^-)$	7; 13	$E_i + 0.01$	2.1×10^{-12}	3.5×10^{-13}	6.0	+1.282	[7a]	
Mn_i^{++}	7	$E_i - 0.21$			23.1 (18.5÷28.3)	+1.57	[7a]	
all Mn Traps	7	$\sigma = (\sigma_{min} \cdot \sigma_{max})^{1/2} \approx 1.0 \times 10^{-15}$; $\sigma_{max}/\sigma_{min} \sim 10^6$					[5c], [7a]	6400
Fe_i^+	8	$E_i - 0.16$	5.0×10^{-14}	7.0×10^{-17}	714.3	+3.286	[7d]	

$(Fe_i^+ B_s^+)$	8; 13	$E_i + 0.28$ (± 0.02)	1.4×10^{-14} (± 0.02)	1.1×10^{-15} ($0.5 \div 2.5$)	13	+1.282	[7c]	
Co_i^+	9	$E_i - 0.02$	$\sigma = (\sigma_n \cdot \sigma_p)^{1/2} \approx 6.6 \times 10^{-15}$				[5c]	3700
Ni_i^+	10							
Pt_s^-	10	$E_i + 0.31$	3.4×10^{-15}				[11]	
Pt_i^-	10	$E_i + 0.02$	4.5×10^{-15}	1.09×10^{-14}	<u>2.42</u>	<u>+0.442</u>	[11]	970
Pt_s^+	10	$E_i - 0.18$		5.4×10^{-14}			[11]	
Au_s^-	11	$E_i - 0.01$	1.4×10^{-16}	7.6×10^{-15}	0.01842	-1.997	[7d]	
			5.0×10^{-16}	1.0×10^{-15} $\propto T^{-4}$	0.5	-0.3466	[12c]	565
Zn_s^-	12	$E_i + 0.07$	1.3×10^{-19}	6.6×10^{-15}	1.97×10^{-5}	-5.417	[7d]	
Zn_s^-	12	$E_i - 0.21$	1.5×10^{-15}	4.4×10^{-15}	0.3409	-0.538	[7d]	
$PV_p \equiv$ $E\text{-center}$	14	$E_i + 0.10$	$\sigma = (\sigma_n \cdot \sigma_p)^{1/2} \approx 6.6 \times 10^{-15}$				[13a]	70
		$E_i + 0.084$	3.7×10^{-16}				[13b]	
PV^+	14	$E_i - 0.27$					[13a]	1.8

From Table 2 (see e.g. the results referring to the traps Cr_i^{++} , Mo_i^+ , Au_s^- , $PV\text{-pair} \equiv$ acceptor E-center), there result also the accuracies (not too good) of the capture cross-sections evaluations, and of their polarization degree. One finds also that the recombination rate U was not still measured systematically. Given being the capture cross-sections and their polarization degree pdg are often temperature dependent, table 3 synthesizes the main types of the temperature dependence of the capture cross-sections.

Table 3. Main types of the temperature dependence of the capture cross sections of free electrons and/or holes, respectively in different semiconductors

The type of the temperature dependence	Typical expression of temperature dependence	Some examples for the traps in the semiconductor	Reference
Arrhenius law	$\sigma_n(T) \approx \sigma_{n\infty} \exp(-E_B/kT)$	EL2, HL1, HL10 in GaAs	[14a]
Power laws	$\sigma(T) \propto T^{-n}$	$n \approx 0.21$ ($\sigma_{n, Au}$ in n -Si)	[12d]
		$n \approx 2.5$ ($\sigma_{n, Au}$ in p -Si)	[12c]
		$n \approx 4.0$ ($\sigma_{p, Au}$ in n -Si)	[12c]
Temperature independence	$\sigma(T) \approx \text{constant}$	σ_p in GaAs	[14a]
		$\sigma_{n, Au}$ in n -Si	[12c]

5. Experimental evaluation of the difference $E_t - E_i$

In order to interpret the obtained (calculated) values of $E_t - E_i$ corresponding sometimes to a mixture of defects inside each studied pixel, an experimental evaluation of the difference $E_t - E_i$ is necessary. Given being that the most efficient experimental method intended to the defects location inside the studied semiconductor forbidden band is the deep-level transient spectroscopy (DLTS) method, we have to evaluate the $E_t - E_i$ difference starting from the defects (traps) positions relative to the upper limit E_v of the valence band and the bottom limit (edge) E_c of the conduction one (see fig. 2).

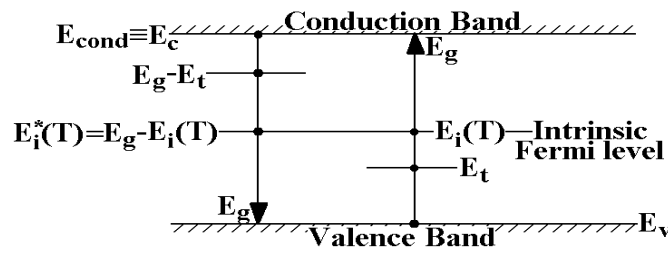


Fig. 2. Positions of the defects (traps) energy levels and of the Fermi intrinsic level according to the DLTS results.

Given being for a certain temperature T the energy gap is (approximately) known, it is necessary to evaluate also the intrinsic Fermi energy $E_i(T)$ at this temperature. According to the basic Condensed Matter Physics treatises [2], the temperature dependence of the intrinsic Fermi energy $E_i(T)$ is given by the expression:

$$E_i(T) = \frac{1}{2} E_g(T) + \frac{3kT}{4} \ln \frac{m_{dp}^*}{m_{dn}^*}, \quad (8)$$

where:

$$m_{dp}^* = \left[m_{pl}^{*3/2} + m_{ph}^{*3/2} \right]^{2/3} \quad \text{and:} \quad m_{dn}^* = \sqrt[3]{6m_t^{*2} \cdot m_l^*} \quad (9)$$

are the effective masses corresponding to the states densities of holes and free electrons, respectively, while m_{pl}^* , m_{ph}^* , m_l^* and m_t^* are the effective masses associated to the light and heavy holes, respectively, and to the longitudinal and transverse electrons effective masses, relative to the major axis of the energy ellipsoid $E(\bar{k})$. For free electrons in silicon, there are used the values $m_l^* = 0.98 m_o$, $m_t^* = 0.19 m_o$, and $m_l^* = 0.916 m_o$, $m_t^* = 0.225 m_o$, which lead to the values $m_{dn1}^* \cong 0.5965 m_o$ and $m_{dn2}^* \cong 0.6528 m_o$ of the effective mass

associated to the electrons state density in the conduction band of *Si*, while for the holes from *Si* there are usually used the values $m_{pl}^* = 0.16 m_o$, $m_{ph}^* = 0.49 m_o$, which lead to the value $m_{dp}^* \cong 0.5492 m_o$ of the effective mass associated to the holes state density in the silicon valence band. As we use the first or the second

pair of electron effective mass in *Si*, we obtain $\frac{3}{4} \ln \frac{m_{dp}^*}{m_{dn}^*} \cong -0.06196$, or -0.1296 ,

hence the temperature coefficient of the silicon intrinsic Fermi energy correction:

$\left| \frac{3k}{4} \ln \frac{m_{dp}^*}{m_{dn}^*} \right| \leq 1.116 \times 10^{-5} K^{-1}$ is at least one magnitude order less than that of the

energy gap corresponding to silicon: $E_{g,Si}(T) \cong 1.21 - 4.2 \times 10^{-4} T$ (eV) [2].

For an average use temperature $T \approx 250$ K (this work, [12a], etc.), one finds that

the intrinsic Fermi energy correction $\frac{3kT}{4} \ln \frac{m_{dp}^*}{m_{dn}^*}$ has a value inside the interval

(1.34; 2.8) meV, remaining so negligible relative to the usual defects (traps) energies in *Si*, even for the very-deep level defects, detectable by the studied dark current spectroscopy method.

6. On the evaluation of the polarization degree of capture cross-sections of free electrons and holes, respectively

Taking into account that the power law expressions of the temperature dependence of capture cross-sections can be approximated by Arrhenius type expressions (with negative activation energy E_B) and substituting the Arrhenius expression [see Table 3] in the polarization degree definition (7), one obtains:

$$pdg(T) = \frac{1}{2} \ln \frac{\sigma_n(T)}{\sigma_p(T)} = \frac{1}{2} \ln \frac{\sigma_{n\infty}}{\sigma_p} - \frac{E_B}{2kT} = pdg_\infty - \frac{E_B}{2kT},$$

hence the temperature dependence of the hyperbolic secant argument can be expressed as:

$$\arg \operatorname{sech}(T) = \frac{E_t - E_i}{kT} + pdg(T) = \frac{E_t - E_i - E_B/2}{kT} + pdg_\infty = \frac{(E_t - E_i)_{eff}}{kT} + pdg_\infty, \quad (10)$$

by means of the effective energies difference $(E_t - E_i)_{eff}$ and of the $pdg(T)$ asymptotic value pdg_∞ .

The DCS method allows however an indirect evaluation of the ‘‘polarization degree’’ pdg (in fact of its asymptotic value pdg_∞), starting from the improved

approximation (5). Our (indirect) evaluation of the effective parameters $|E_t - E_i|_{\text{eff}}$ and pdg_∞ was achieved by means of the least-squares fit (using the gradient method) of the slope s and intercept i of the regression line of the modulus of the argument of the hyperbolic secant function in terms of the $\frac{1}{kT}$ parameter:

$$\left| \arg \left[\operatorname{sech} \left(\frac{E_t - E_i}{kT} + pdg \right) \right] \right| = s \cdot \frac{1}{kT} + i. \quad (11)$$

In order to provide correct interpretations of the results of our procedure (10), we studied the existing experimental data for 20 randomly chosen pixels of a Spectra Video CCD camera (model SV512V1) manufactured by Pixelvision, Inc. (see [9a]). The obtained (in the frame of this work) types of qualitative results and their interpretations are synthesized by Table 4.

Table 4. Main types of results obtained by means of the regression line $|\arg[\operatorname{sech}(pdg + (E_t - E_i)/kT)] = i + s/kT$ study and their interpretation

Slope s sign	Intercept i sign	Interpretation	Examples of pixels [12a]
> 0	> 0	Both $(E_t - E_i)_{\text{eff}}$ and pdg_∞ have the same sign, hence: $ E_t - E_i _{\text{eff}} = s$, $pdg_\infty = i$ and: $(E_t - E_i)_{\text{eff}}/pdg_\infty > 0$	188; 471
> 0	< 0	$(E_t - E_i)_{\text{eff}}/kT > -pdg_\infty > 0$ or $(E_t - E_i)_{\text{eff}}/kT < -pdg_\infty < 0$	121; 200
< 0	> 0	$pdg_\infty > -(E_t - E_i)_{\text{eff}}/kT = (E_i - E_t)_{\text{eff}}/kT > 0$ or $pdg_\infty < -(E_t - E_i)_{\text{eff}}/kT = (E_i - E_t)_{\text{eff}}/kT < 0$	321; 400

In order to estimate the “impact” of the polarization degree (pdg) values on the depletion dark current the obtained numerical results for the 17 pixels whose data sets lead to physically convergent evaluations were synthesized by Table 5. As one can find easily, the accuracy of the obtained results decreases very much for the pixels emitting weak depletion dark current (low values of the depletion pre-exponential factor, Dep).

Table 5. Interpretation of the obtained quantitative (numerical) results [$s = \operatorname{sign}(E_t - E_i)_{\text{eff}}$]

Pixel	Dep (Mcps·K ^{-3/2}), 10 ⁶ counts/s·K ^{-3/2}	Obtained information about the effective parameters		Calc. Depletion Dark Current Accuracy (%)	sech[$pdg +$ $(E_t - E_i)/kT$]
		$ E_t - E_i _{\text{eff}}$, meV	$s \cdot pdg_\infty$		
321; 400	2.541	32.125	-3.075	17.47%	0.3808
181; 260	5.433	24.39	0.0187	2.975%	0.5887
121; 200	6.022	34.44	-0.3274	5.65%	0.5381
141; 220	6.478	8.49	0.773	6.158%	0.5872
101; 180	6.623	24.66	0.0455	2.454%	0.5702

301; 380	7.224	30.85	-0.3114	3.002%	0.6068
188; 471	9.530	28.04	0.790	6.988%	0.2511
81; 160	11.710	33.59	0.0154	2.294%	0.4117
221; 300	15.998	28.03	0.438	3.797%	0.2176
201; 280	21.944	31.21	0.117	1.77%	0.4140
29; 88	32.120	51.860	-0.155	2.473%	0.2207
61; 140	40.792	27.352	1.369	7.055%	0.1467
281; 360	66.386	45.697	0.397	3.197%	0.1688
261; 340	105.688	57.225	0.135	2.2798%	0.1306
341; 420	254.039	55.479	0.259	2.277%	0.1249
161; 240	268.671	76.223	0.632	3.73%	0.0338
31; 247	421.361	2.16	-1.3896	5.379%	0.5109

Figures 3 and 4 present the diagrams of the traps levels for *GaAs* and *Mn* in the *Si* lattice, respectively. From Table 2, one finds that the majority of donor /acceptor states are located in the upper/lower half of the forbidden band, respectively, while the other states – named here “trans-Fermi level donor/ acceptor states” (as the levels *EL2*, *E5*, *HL10*, *HL16* in *GaAs*, $(Mn^+Au^-)^+$ and Mn_i^{++} in the *Si* lattice) have negative values of the product $pdg \cdot \text{sign}(E_i - E_f)$.

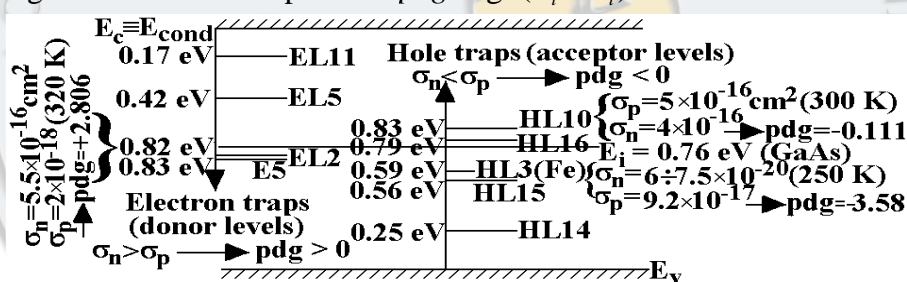


Fig. 3. Traps levels diagram for GaAs [14a].

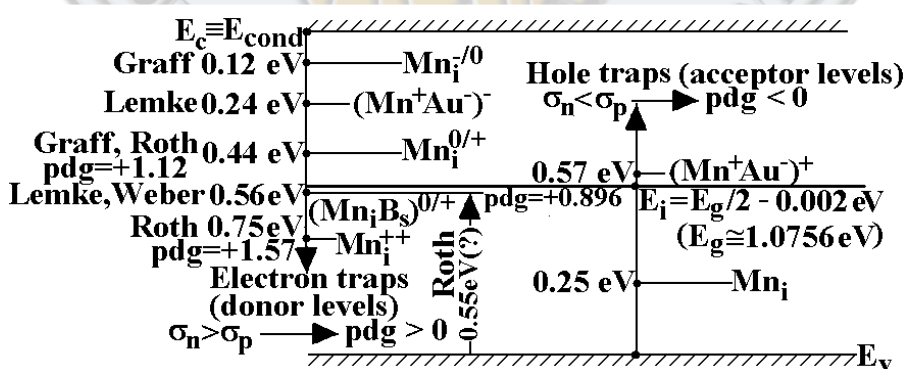


Fig. 4. Traps levels diagram for Mn in the silicon lattice [7, 8, 15].

Taking into account that the number of the “trans-Fermi level states” is sensibly less than the number of the other electronic states, this finding represents a useful tool in the assignment of these states (traps).

6. Study of the “anomalies” of the generation rate U values

This work achieved the least-squares fit (using the gradient method [17], [16b]) of the improved approximation (5):

$$De^- = De_{0,diff}^- T^3 \exp\left(-\frac{E_g}{kT}\right) + De_{0,dep}^- T^{3/2} \exp\left(-\frac{E_g}{2kT}\right) \operatorname{sech}\left[\frac{(E_t - E_i)_{eff}}{kT} + pdg_\infty\right]$$

of the experimental results concerning the dark current emitted by some pixels of the studied Spectra Video CCD camera (model SV512V1) [12a].

There were obtained evaluations of all parameters of the above expression, particularly of the depletion pre-exponential factor $De_{0,dep}^- \equiv Dep$, effective energy gap E_g and of the trap location $(E_t - E_i)_{eff}$ inside the silicon forbidden band, as well as of the asymptotic value pdg_∞ of the capture cross-sections polarization degree. Using these numerical estimations, the numerical evaluation of the generation rate at the temperature $t_{gr} = 55^\circ\text{C}$ (hence $T_{gr} = 328.15\text{ K}$) was obtained by means of the expression:

$$U(T_{gr}) = De_{0,dep}^- T_{gr}^{3/2} \exp\left(-\frac{E_g}{2kT_{gr}}\right) \cdot \operatorname{sech}\left[\frac{(E_t - E_i)_{eff}}{kT_{gr}} + pdg_\infty\right]. \quad (12)$$

The obtained results are presented in Table 6, where the pixels were written in the monotonic order of their increasing depletion pre-exponential factors Dep . While – according to the classical approximation (4) – it was expected to find the proportionality of the generation rate $U(T)$ with the depletion pre-exponential factor $Dep \equiv De_{0,dep}^-$, the examination of Table 6 points out several discontinuities, that can be explained only by the different values of polarization degree pdg_∞ and of the effective energies difference $(E_t - E_i)_{eff}$.

Table 6. Comparison of the evaluated values of the depletion pre-exponential factor Dep and of the generation rate (corresponding hyperbolic secant function values in brackets) for different pixels of a Spectra Video CCD camera (model SV512V1)

Pixel	Dep (Mcps $\text{K}^{-3/2}$), $10^6 \text{ counts/s} \cdot \text{K}^{-3/2}$	Evaluated generation rate $U(\text{e}^-/\text{s})$ at 55°C	Pixel	Dep (Mcps $\text{K}^{-3/2}$), $10^6 \text{ counts/s} \cdot \text{K}^{-3/2}$	Evaluated generation rate $U(\text{e}^-/\text{s})$ at 55°C
321; 400	2.541	124.6 (0.3808)	201; 280	21.944	2243 (0.4140)
181; 260	5.433	680 (0.5887)	29; 88	32.120	1981 (0.2207)

121; 200	6.022	866 (0.5381)	61; 140	40.792	1464 (0.1467)
141; 220	6.478	713.5 (0.5872)	281; 360	66.386	3184 (0.1688)
101; 180	6.623	751 (0.5702)	261; 340	105.688	3276 (0.1306)
301; 380	7.224	1564 (0.6068)	341; 420	254.039	3899 (0.1249)
188; 471	9.530	588 (0.2511)	161; 240	268.671	1996 (0.0338)
81; 160	11.710	1176 (0.4117)	31; 247	421.361	4923 (0.5109)
221; 300	15.998	1654 (0.2176)			

The considerable impact of the polarization degree (pdg) on the values of the hyperbolic secant $\sec h \left[\frac{(E_t - E_i)_{eff}}{kT} + pdg_{\infty} \right]$ and of the generation rate, is indicated both by the values of the last column of Table 5 (see the value for the pixel 161; 240, particularly) and of Fig. 1.

According to the work [5c], the even more striking large generation rates of the Mn , Ni , Co traps (see e.g. Table 1) could be explained by means of a complex character (like Mn_4) of these traps and/or of a possible Poole-Frenkel [18] effect. The accomplished analysis pointed out that even the capture cross-sections of the Ni and Co traps are considerably larger than that of the substitutional gold Au_s , their generation rates agree very well [according to the classical approximation (4), see Table 1, with that of Au_s , while even the use of the improved approximation (5) does not lead to a quantitative justification of the experimental value of the Mn trap generation rate.

Given being the: a) considerably more complex defect structure (larger number of charge states) of Mn than those of Cr , Fe , Ni , Co , etc, b) still incompletely characterized (mainly by means of the capture cross sections of free electrons and holes, respectively) of many Mn defects (e.g. of the substitutional states, of the Mn_4 cluster, of the Mn pairs with Al , Ga , Sn , etc), c) intentional contamination with Mn atoms which lead to the McColgin's results [5c], our analysis lead to the conclusion that the striking strange pair of values referring to the average cross-section σ and to the generation rate/ Mn atom can be explained (more than by the Poole-Frenkel effect) by an averaging of the generation rates of Mn defects in different charge states with very different capture cross sections (many of them considerably higher than the average value indicated by [5c]).

The obtainment of new experimental information about both free electrons σ_n and holes σ_p capture cross-sections of the main deep-level traps in silicon will contribute of course to a more accurate description of the temperature dependence of the depletion dark current in semiconductors.

7. Use of the polarization degree pdg as an assignment criterion of the deep-level traps

The accomplished study pointed out that the newly defined physical parameter “polarization degree of the capture cross-sections of free electrons and holes, respectively” is a basic feature of the deep-level traps, allowing considerably more accurate descriptions of the temperature dependence of the depletion dark current in charge-coupled devices.

For this reason, we consider that besides the classical assignment criteria as the: a) depletion pre-exponential factor $De_{0,dep}^-$, b) generation rate $U(T_{g.r.})$ at a given temperature, c) the location of the studied trap inside the semiconductor forbidden band, d) average capture cross-section $\sigma \equiv \sigma_{ave} = \sqrt{\sigma_n \sigma_p}$, the: e) polarization

degree $pdg = \frac{1}{2} \ln \frac{\sigma_n}{\sigma_p} = \arg \tanh \frac{\sigma_n - \sigma_p}{\sigma_n + \sigma_p}$ of capture cross-sections, as well as the:

f) average value $\text{sech}[(E_t - E_i)_{eff} / kT_{ave} + pdg_{\infty}]$ of the hyperbolic secant function, are also basic assignment criteria for the deep-level traps in a semiconductor, starting from the observed temperature dependence of the dark current in each CCD pixel (the Dark Current Spectroscopy method).

Conclusions

This work pointed out the necessity to introduce the new parameter “polarization degree of the capture cross-sections of free electrons and holes, respectively” in order to ensure a sufficiently accurate description of the temperature dependence of the depletion dark current in semiconductors. It was found also the ability of this new parameter to: a) analyze successfully the “anomalies” of some reported generation rate values [e.g., no anomaly for the reported generation rates of *Ni* and *Co* [5c], but probably wrong value ($1 \div 2 \times 10^{-14} \text{ cm}^2$, instead of $\sim 1 \times 10^{-15} \text{ cm}^2$) for the average cross-section of the electronic states of the embedded *Mn* traps which produce a 6400 e^-/s generation rate], b) discriminate among the contributions of the different deep-level traps to the depletion dark current in each CCD pixel, allowing so certain assignments of the deep-level traps in the CCDs pixels. In this aim, both newly introduced notions of “polarization degree” and “trans-Fermi level donor/acceptor states” are useful.

Acknowledgements

The authors thank very much for the fruitful discussions and important received information to Dr. G. Moagar-Paladian, National Institute for Research and Development in Micro-technology, Bucharest.

REFERENCES

- [1] C. Sah, R. Noyce, W. Shockley, Carrier Generation and Recombination in p-n Junction and p-n Junction Characteristics, in Proc. IRE, **vol. 45**, 1957, p. 1228.
- [2] a) A. S. Grove, Physics and Technology of Semiconductor Devices, New York, Wiley, 1967; b) S. M. Sze, Physics of Semiconductor Devices, New York, Wiley, 1981; c) I. Munteanu, Fizica stării condensate, Editura Hyperion, București, 1995.
- [3] R. Widenhorn, M. M. Blouke, A. Weber, A. Rest, E. Bodegom, Temperature dependence of dark current in a CCD, in Proc. SPIE Int. Soc. Opt. Eng., **vol. 4669**, 2002, pp. 193-201.
- [4] R. D. McGrath, J. Doty, G. Lupino, G. Ricker, J. Vallerga, Counting of Deep-Level Traps using a Charge-Coupled Device, in IEEE Trans. on Electron Devices, **vol. ED-34**, no. 12, 1987, pp. 2555-2557.
- [5] a) W. C. McColgin, J. P. Lavine, J. Kyan, D. N. Nichols, C. V. Stancampiano, Dark Current Quantization in CCD Image sensors, in Proc. Int. Electron Device Meeting, pp. 113-116, 13-16 December 1992; b) W. C. McColgin, J. P. Lavine, C. V. Stancampiano, Probing metal defects in CCD image sensors, in Proc. Mat. Res. Soc. Symp., **vol. 378**, pp. 713-724, 1995; c) W. C. McColgin, J. P. Lavine, C. V. Stancampiano, J. R. Russell, Deep-level traps in CCD image sensors, in Proc. Mat. Res. Soc. Symp., **vol. 510**, pp. 475-480, 1998.
- [6] J. R. Janesick, Scientific Charge-Coupled Devices, SPIE Press, The International Society for Optical Engineering, Bellingham, Washington, 2001.
- [7] a) T. Roth, P. Rosenitz, S. Diez, S. W. Glunz, D. McDonald, S. Beljakowa, G. Pensl, Electronic properties and dopant pairing behavior of manganese in boron-doped silicon, in J. Appl. Physics, **102**, 103716-8, November 2007; b) P. Rosenitz, T. Roth, S. Diez, D. McDonald, S. W. Glunz, Detailed studies of manganese in silicon using lifetime spectroscopy and deep-level transient spectroscopy, Proc. 22nd Eur. Conf. Photo-voltaic Solar Energy, EU-PVSEC 2007, Milan, Italy, 3-7 September 2007, pp. 1480-1483(2007); c) J. E. Birkholz, K. Bothe, D. McDonald, J. Schmidt, Electronic properties of iron-boron pairs in crystalline silicon by temperature- and injection-level-dependent lifetime measurements, in J. Appl. Phys., **vol. 97**, 2005, 103708; d) D. McDonald, L. J. Geerligs, Recombination activity of interstitial iron and other transition metal point defects in p- and n-type crystalline silicon, in Appl. Phys. Lett., **vol. 85**, no. 18, November 2004, pp. 4061-4063.
- [8] a) K. Graff, Metal impurities in silicon-device fabrication, **vol. 24**, Springer, Berlin, 1999; b) S. Rein, Lifetime spectroscopy: a method of defect characterization in Si for photo-voltaic applications, Springer, Berlin, 2005.
- [9] D. V. Lang, Deep-level transient spectroscopy: A new method to characterize traps in semiconductors, in Journ. Appl. Physics, **vol. 45**, no. 7, July 1974, pp. 3023-3032.
- [10] a) J. Schmidt, R. Krain, K. Bothe, G. Pensl, S. Beljakava, Recombination activity of interstitial chromium and chromium-boron pairs in Si, in J. Appl. Phys., **vol. 102**, 2007, 123701; b) B. B. Pondyal, K. R. McIntosh, D. H. McDonald, G. Coletti, Temperature dependent e^- and h^+ capture cross sections of Mo in silicon, Proc. 24th European Photo-voltaic Solar Energy Conf., 21-25 September 2009, Germany.

- [11] Y. K. Kwon, T. Ishikawa, H. Kuwano, Properties of platinum-associated deep levels in silicon, in *J. Appl. Phys.*, vol. **63**, February 1987, pp. 1055-1058.
- [12] a) A. G. Nassibian, L. Faraone, Capture cross section of gold in silicon, in *Appl. Phys. Letters*, vol. **33**, 1978, p. 451; b) W. D. Davis, Lifetimes and capture cross sections in gold-doped silicon, in *Phys. Rev.*, vol. **114**, 1959, pp. 1006-1008; c) G. Bemski, Recombination properties of gold in silicon, in *Phys. Rev.*, vol. **111**, 1958, pp. 1515-1518; d) J. Barbolla, M. Pugnet, J. C. Brabant, M. Brousseau, Thermal capture cross section of free electrons at neutral gold centres in n-type silicon, in *Phys. stat. sol. (a)*, vol. **36**, no. 2, 1976, pp. 495-498.
- [13] a) A. N. Larsen, A. Mesli, The hidden secrets of the E-centre in Si and Ge, in *Physica B*, vol. **401-402**, 2007, pp. 85-90; b) J. B. Spratt, B. C. Passenheim, R. E. Leadon, The effects of nuclear radiation on P-channel CCD imagers, *Proc. Radiation Effects Data Workshop, IEEE*, 1997, pp. 116-121.
- [14] a) A. Mitonneau, A. Mircea, G. M. Martin, D. Pons, Electron and hole capture cross-sections at deep centres in gallium arsenide, *Rev. Phys. Appliquée*, vol. **14**, October 1979, pp. 853-861; b) D. V. Lang, R. A. Logan, in *J. Electron. Mat.*, vol. **4**, 1975, p. 1053; c) C. H. Henry, D. V. Lang, in *Phys. Rev. B*, vol. **13**, 1977, p. 989; d) P. E. Sterian, R. Rogojan, A. R. Sterian, Alumino-phosphate semiconductor, *Proc. SPIE "Laser Physics and Applications"*, **4394**, 2001, pp. 358-361.
- [15] a) H. Lemke, Energieniveaus und Bindungsenergien von Ionenpaaren in Silizium, in *Phys. Stat. Sol. (a)* vol. **76**, 223-234(1983); b) H. Lemke, Eigenschaften einiger Störstellen-komplexe von Gold in Silizium, in *Phys. Stat. Sol. (a)* vol. **75**, 473-482(1983); c) E. R. Weber, Transition Metals in Silicon, in *Appl. Phys.*, vol. **A30**, 1-22(1983).
- [16] a) R. Widenhorn, E. Bodegom, D. Iordache, I. Tunaru, Computational Approach to Dark Current Spectroscopy in CCDs as Complex Systems. I. Experimental Part and Choice of the Uniqueness Parameters", in the Scientific Bulletin of "Politehnica" University Bucharest, Series A: Applied Mathematics and Physics, vol. **72**, no. 4, 2010, pp. 197-208; b) I. Tunaru, R. Widenhorn, D. Iordache, E. Bodegom, *ibid.* II. Numerical Analysis of the Uniqueness Parameters Evaluation, *ibid.*, **73**(1) 149-162(2011).
- [17] a) K. Levenberg, A method for the solution of certain problems in least squares, *Quarterly of Applied Mathematics*, vol. **2**, 1944, pp. 164-168; b) D. W. Marquardt, An algorithm for least-squares estimation of nonlinear parameters, *Journal of the Society for Industrial and Applied Mathematics*, vol. **11**, no. 2, 1963, pp. 431-441; c) N. Andrei, Another Conjugate Gradient Algorithm for Unconstrained Optimization, *Annals of the Academy of Romanian Scientists, Series on Science and Technology of Information*, vol. **1**, no. 1, 2008, pp. 7-20.
- [18] A. Sevenco, Gh. Brezeanu, An accurate analytical model with a reduced parameter set for short-channel MOS transistors, *Annals of the Academy of Romanian Scientists, Series on Science and Technology of Information*, vol. **2**, no. 1, 2009, pp. 107-120.
- [19] a) J. Frenkel, On pre-breakdown phenomena in insulators and semiconductors, in *Phys. Rev.* vol. **54**, 1938, p. 647; b) J. van der Spiegel, G. J. Declerk, Characterization of Dark Current Non-Uniformities in CCDs, in *Solid-State Electronics*, vol. **27**(2) 1984, pp. 147-154; c) W. E. Meyer, Digital DLTS studies on radiation induced defects in Si, GaAs and GaN, PhD Diss., Univ. of Pretoria (South-Africa), Nov. 2006; d) E. A. G. Webster, R. Nicol, L. Grant, D. Renshaw, Validated Dark Spectroscopy on a per-pixel basis in a CMOS image sensors, *Proc. International Image Sensor Workshop, Bergen (Norway)*, 26-28 July 2009.
- [20] A. Danchiv, M. Bodea, Cl. Dan, Chopper Stabilization Techniques, part I: Chopper Amplifier Topologies Overview, *Annals of the Academy of Romanian Scientists, Series on Science and Technology of Information*, vol. **1**, no. 1, 2008, pp. 31-42.